

A Novel Compliant Rover for Rough Terrain Mobility

Arun Kumar Singh, Rahul Kumar Namdev, Vijay Eathakota, K.Madhava Krishna

Abstract—In this paper a novel suspension mechanism for rough terrain mobility is proposed. The proposed mechanism is simpler than the existing suspension mechanism in the sense that the number of links and joints has been significantly reduced without compromising the climbing ability of the rover. We explore the use of compliant elements like springs for passively controlling the degree of freedom of the proposed mechanism and a framework for optimizing the spring parameters has been proposed. A performance evaluation of the proposed mechanism has been shown in terms of extensive simulations.

I. INTRODUCTION

To design an effective suspension mechanism with minimum design and control complexity is the focus of the research here. Past research on wheeled all terrain vehicles has led to the development of two types of suspension mechanisms: active and passive. Passive suspension rovers adapt passively to the underlying terrain by the virtue of contact forces and do not require any actuators for controlling the internal configuration of the vehicle significantly reducing the control architecture. Rocky7[1] is one such vehicle which utilizes one of the simplest suspension mechanisms called rocker bogie. But the climbing ability and specially the lateral stability is limited as compared to shrimp[2] which utilizes a more sophisticated design derived from the four bar mechanism to enhance climbing ability. But as sophistication increases the number of joints and links also increase, increasing the overall complexity and weight of the system. In general joints are heavy parts and can easily lead to trouble in space environments [3]. Passive suspension rovers are usually multi wheel drive system [MWD] e.g. some rovers such as Lunokhod [4] and Marshakhod [5] have 6 or more wheels. Though the system has higher degree of mobility the system is intended to be heavier and hence not ideally applicable to medium to small scale rovers. Moreover the closed kinematic structures of passive suspension rovers pose additional constraint on the kinematic analysis and motion planning of the robot. Active suspension rovers on the other hand are based mainly on open kinematic joints which are simple but require actuators to maintain static stability of the system. One such system named Hylos [6] requires 8 actuators to control its internal configuration of four 2dof leg. But simplicity in the kinematic structure has to be compensated by increasing the complexity at the control architecture level.

In our work we propose a four-wheeled passive suspension capable of traversing uneven terrain including steps. Four-wheeled passive step climbers are rare and hence the proposed mechanism enjoys uniqueness in design and implementation. We explore the use of compliant elements like springs for controlling the internal *dof* (degree of freedom) of the suspension mechanism. Use of compliant elements to passively control the internal *dof* of the mechanism is the key novelty of this paper. The mechanism adapts passively to the terrain undulations. This simplifies the control complexity of the rover and even makes open loop operation possible. The use of springs for rough terrain mobility has been proposed in [7] but the essence of compliance was not fully exploited in the sense that such systems as proposed in [7] could work without springs as well. A comparative study has been performed between a rigid suspension vehicle and the proposed suspension to show the effect of compliance in improving the terrain adaptability. The vehicle performance has been analyzed for step climbing and spring parameters have been tuned for such obstacles. It is shown with the help of simulations that the spring parameters tuned for step like obstacle works well for irregular terrain without discontinuities as well.

II. KINEMATIC MODEL OF THE PROPOSED MECHANISM

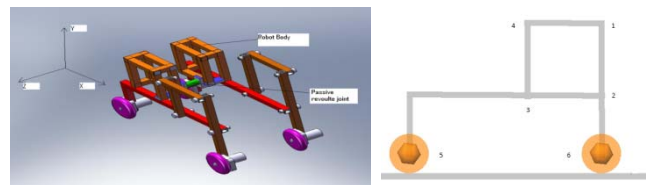


Fig.1(left). CAD Model of the Suspension Mechanism. **Fig.2 (right).** Front View of the suspension mechanism

Figure.1 and 2 shows the isometric and front view of the kinematic model of the proposed suspension mechanism. The mechanism is derived from planar four-bar mechanism. The rover has two planar mechanisms connected by a revolute joint in between. The revolute joint helps the rover to maintain wheel ground contact even when both the halves of the suspension are operating on different surfaces. This is important for stability and is an enhancement over conventional differential gearing arrangement employed in [1],[9] because it decouples the dynamics of both the halves in the pitch plane. This however requires that the robot body

should be attached separately to both the halves as shown in figure.1. Considering shrimp [2] as the bench-mark mechanism is designed with the objective of reducing the number of links, joints and wheels without reducing the overall climbing ability of the mechanism. Proposed mechanism can still climb steps and navigate over irregular terrains without discontinuities as well and hence comes as a promising candidate for the suspension design. Shrimp design found in [2] employs 18 bodies and 22 joints while the proposed mechanism employs 14 bodies and 13 joints. All the numbered joints shown in figure.2 are revolute and since the mechanism is planar the wheel ground contact point can be modeled as a 1dof revolute joint [8] Reduction in joints has major benefits because it leads to the reduction in the overall weight of the rover and in turn leading to the possibility of usage of smaller actuators. However changing number of joints is critical task as the internal dof of the suspension mechanism is dependent on the number of joints. For the existing suspension mechanisms the number of joints is so chosen that the internal dof of the mechanism becomes 1 to ensure static equilibrium [1],[2]. Mechanisms having internal dof greater than 1 possess internal self motions and hence have to include additional constraints to maintain equilibrium [11]. Thus the proposed suspension mechanism is fundamentally different from the existing suspension mechanisms because the internal mobility as given by grubler's criterion comes out to be $2(N = 7, J = 8, Fi = 8)$. So one actuator is needed to control the internal configuration of the mechanism. The previous experiments with this mechanism incorporated a velocity controlled motor at joint 4 [9]. But the present work is aimed at reducing the actuation requirement and simplifying control architectures to enable open loop operation of the rover. Hence we replace the velocity controlled motor from [9] with a torsion spring at joint 4. Thus in principal the mechanism is under-actuated. We show in the later sections that the motion of the complaint joint can be appropriately controlled with the help of wheel-ground interaction and wheel motor torques. This is a critical difference between the usage of compliant elements in the proposed mechanism and in [7]. Moreover the mechanism also uses less number of wheels and is shown in the later sections that for the proposed mechanism four wheels are enough to generate sufficient normal force for climbing step-like discontinuities. Introduction of compliance in the form of springs enables proper traction and normal force distribution among the wheels but poses additional design complexity in terms of optimizing the spring parameters. These are described in the subsequent sections

III. EFFECT OF SPRING COMPLIANCE ON NORMAL FORCE DISTRIBUTION

To show the effect of compliance we carried out some simulation tests on the proposed mechanism with one of its revolute joints being locked. The mechanism in this case becomes as structure or in other words a rigid suspension vehicle and its causes of failure of the rigid model point is analyzed. Figure.3 shows the vehicle in contact with a step like obstacle.

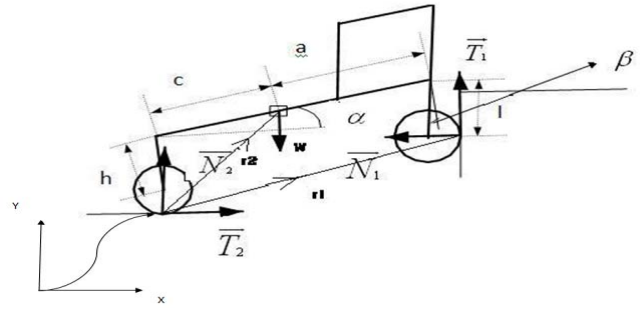


Figure.3. Rover in contact with a step like obstacle

When the front wheel is climbing the obstacle, the normal reaction force from the obstacle is horizontal and does not involve any contribution from the weight of the rover. The normal force \vec{N}_1 is critical for the rover to cross over the obstacle because the available traction force \vec{T}_1 is a function of \vec{N}_1 . Hence the wheel should always be in contact with the surface of the obstacle. Larger the value of \vec{N}_1 bigger the no-slip margin and hence larger values of torques can be commanded from the motor without incurring slip. Considering the situation in the figure the following equation holds true

$$\vec{T}_2 = \vec{N}_1 \quad (1)$$

This means the traction force at the back wheel \vec{T}_2 is responsible for controlling \vec{N}_1 and hence should be effectively transferred to the front wheel which calls for the following two conditions.

1. The front wheels should always be in contact with the surface of the obstacle so that sufficient normal forces required can be created.
2. The slip should be minimized on all the wheels. This is extremely critical because when the front wheels are climbing the obstacles the rear wheels have the maximum probability of slipping. The slipping of the back wheels results in the loss of traction forces and reduction in the transmission of the traction forces from the rear to the front wheels. The slips in the wheels are defined by the slip ratio σ which is given by the following expression

$$\sigma = \begin{cases} 1 - \left(\frac{v}{\omega r}\right) & (\text{Acceleration}) \\ \left(\frac{v}{\omega r}\right) - 1 & (\text{Braking}) \end{cases} \quad (2a)$$

Here r is the radius of the wheel. The effects of both the above cases are coupled and the occurrence of one leads to the other. Figure.4a shows the snapshot of the simulation when a rigid suspension vehicle is encountering a step like obstacle. When the front wheels come in contact with the obstacle, the linear velocity of the wheels is reduced to zero resulting in tremendous wheel-slip. The loss in traction forces due to wheel-slip results in the reduction of the normal forces at the front wheel-ground contact point. This can be seen in figure.5a where the normal forces momentarily goes up when the front wheels comes in

contact with the obstacle but it is not sustained for a sufficient amount of time for the vehicle to climb over it. Figure.6a shows the plot of the slip ratio which shows a value close to 1 from the time the front wheels comes in contact with the obstacle.



Figure.4a(left).Rigid suspension unable to negotiate a step like discontinuity. Figures 4b, 4c. A torsion based suspension mechanism able to negotiate discontinuity

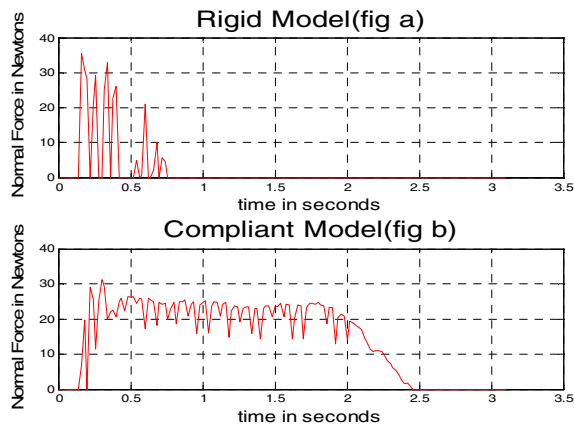


Figure.5. Horizontal component of normal force for all the four wheels

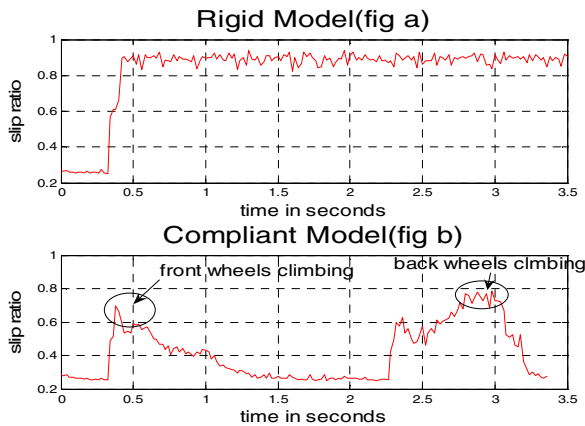


Figure.6. Variation of slip ratio for all the four wheels

The above problem can be solved by introducing compliance in the form of some flexible elements such as springs in the suspension mechanism. To understand this consider figure.7 which shows a rotating wheel connected to a rigid surface with springs.

In figure.7 the wheel rotates and advances forward compressing the spring. The compression in the spring produces the reaction force at the surface. It is to be noted that the above situation is different from the common force control model as found in [10] in the sense that force

developed at the wheel ground contact point \vec{T}_2 depends upon the slip ratio of the wheel which in turn is decided by the amount wheel is moving forward with rotation.

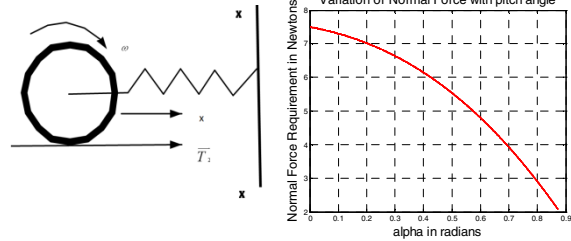


Figure.7(left). Normal Force Control. Figure.8(right). Variation of required N1 with α

The normal reaction force $|\vec{N}|$ produced at the contact surface XX is given by

$$|\vec{N}| = kx + c \frac{dx}{dt} \tag{2b}$$

There are two objectives to be met here (i) improvement in the slip ratio and (ii) Maintaining sufficient normal reaction force at the contact force. Both the objectives are coupled by equation (2b). While theoretically the later can be achieved by any arbitrary value of spring parameters, very high spring stiffness will restrict the forward movement of the wheel resulting in very low value of deformation and its rate and resulting in tremendous wheel slip and consequentially also disturbing the sustenance of the normal reaction force. A rigid suspension is similar to having a spring with extremely high stiffness. This is the main reason why the developed normal reaction force at the front wheel ground contact point could not be sustained in case of rigid suspension vehicle shown earlier in this section. For a particular value of normal force, the very low value of spring parameters will result in very high deformation and significantly improve the slip ratio. However as shown in the later sections, there is a limit to the maximum allowable deformation from the mechanism design point of view. Figure.4b,4c shows the above concept in action. When the suspension mechanism fitted with a torsion spring at joint 4 hits an obstacle, the back wheel does not stop and continues its advancement deforming the spring. Hence the slip and reduction in the traction force is minimized. The deformation in the spring results in a reaction force on the front wheel pushing it against the obstacle. Thus compliance gives a way of transferring the traction forces from the rear wheel to the front wheel and maintaining optimum contact of the wheel and the obstacle. Figure.5b shows the plot of normal forces when the torsion spring based suspension mechanism encounters an obstacle. The plot was obtained by running the rover on open loop with no feedback of required and current normal reaction forces. The motor torque was gradually increased until the rover crossed over the obstacle. It will be shown in the later sections that it is possible to derive analytic expressions which give a measure of the minimum required normal forces at the wheel ground contact point and its relation with the rear wheel motor torques. It can be seen from the plot

that there is a significant improvement in the normal reaction forces. The average normal reaction force developed is increased and is sustained for a longer amount of time. The large normal reaction force resulted in the increment of the no-slip margin and as a consequence of that motor torque could be increased without incurring slip. This is one of the main reasons why the compliance fitted was able to climb over the obstacle. There is an improvement in the slip ratio as well as shown in figure.6b. The slip ratio momentarily goes up for all the four wheels when the front wheels have encountered the obstacle. But it settles down once the rover has started its advancement over the obstacle. The region of high peak corresponds to the time when the four-bar is deforming under the reaction forces from the obstacle. Once the sufficient deformation has taken place to develop adequate normal force, the wheel starts rolling over the obstacle and the wheel slip goes down. Same trend can be seen when the back wheels are climbing over the obstacle.

IV. ESTIMATION OF NORMAL AND TRACTION FORCES

In this section we derive the metric in terms of normal force and coefficient of friction requirement on the wheel-ground contact point for the vehicle to move over a step-like obstacle. Here a planar analysis is presented because it gives better insight into the system dynamics. Referring to figure.3 which shows the FBD of the rover, we can write the following equations

$$\vec{T}_2 = \vec{N}_1 \quad (3), \quad \vec{N}_1 + \vec{T}_2 = W \quad (4)$$

where W is the weight of the rover. In general

$$|\vec{T}_2| \leq \mu |\vec{N}_2| \quad (5) \quad \text{and} \quad |\vec{T}_1| \leq \mu |\vec{N}_1| \quad (6)$$

Equations (5) and (6) are friction cone constraints for the system. In the given situation if the rover has to climb over the obstacle the moments about the contact point 2 should be counter clockwise. We take here the anti-clockwise moment as positive and get the following expression.

$$M_z = \vec{r}_1 \times \vec{T}_1 + \vec{r}_1 \times \vec{N}_1 + \vec{r}_2 \times \vec{W} > 0 \quad (7)$$

Using \vec{r}_1, \vec{r}_2 and the fact that $h = l$ from the dimension of the rover, in equation (7) we get

$$\begin{aligned} & |\vec{N}_1| h \cos(\beta) - |\vec{N}_1| (c + a) \sin(\alpha) + |\vec{N}_1| r + \\ & |\vec{T}_1| (c + a) \cos(\alpha) - |\vec{T}_1| (c + a) \sin(\alpha) \tan(\beta) + |\vec{T}_1| r - \\ & |\vec{T}_1| h \sin(\alpha) - W \cos(\alpha) + W \sin(\alpha) > 0 \end{aligned} \quad (8)$$

Where r is the radius of the wheel.

The above inequality poses a minimum requirement constraint on the normal and traction forces. It can be seen easily that the contribution of $|\vec{N}_1|$ towards producing anticlockwise moment is very less especially at low values of α . Hence the role of $|\vec{T}_1|$ becomes more prominent for the purpose. However $|\vec{T}_1|$ is related to $|\vec{N}_1|$ through the friction-cone inequality (6) which says that with the increase of normal force the traction force developed by the wheel

motor torque can increase. From the above inequality we search for minimum above value of $|\vec{N}_1|$ and $|\vec{T}_1|$ for a given value of weight of the rover and pitch angle α . The weight of the rover in this case was taken to be 60 N. We solve the above problem following a non-linear optimization approach. We frame an objective function as

$$\mu = \min \left\{ \frac{|\vec{T}_1|}{|\vec{N}_1|} \right\} \quad (9)$$

The above objective function infers that we aim to find a solution of inequality that minimizes the ratio of normal to traction forces or in other words minimize the coefficient of friction requirement for climbing over the obstacle.

We frame an additional constraint for the above optimization problem as

$$|\vec{T}_1| r < |\tau_{\max}| \quad (10).$$

Constraint (10) poses an upper bound on the value of $|\vec{T}_1|$ on the basis of saturation value of the wheel motor torques τ_{\max} . Moreover an inequality constraint given by (6) is also a constraint to the above optimization problem

Figure.8 shows the variation of required $|\vec{N}_1|$ as derived from the above optimization problem plotted against the pitch angle. It can be seen from the above plot that the minimum requirement of $|\vec{N}_1|$ decreases with increasing pitch angle α with maximum requirement being at $\alpha = 0$.

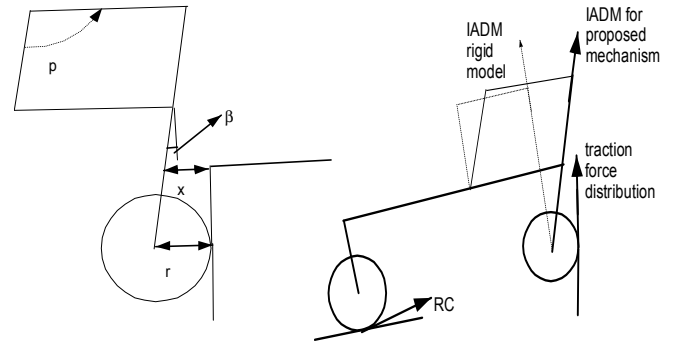


Figure.9(left). Maximum allowable deformation. **Figure.10 (right).** Instantaneous motion direction for front wheel

For a rover to climb over the obstacle, it is not necessary that the normal force variation shown in figure.8 be strictly followed, so long as the developed normal force is more than that required for any given pitch angle. This is because larger normal force than required will only help to generate more traction forces and thus help in satisfying inequality (8). Hence figure.8 gives us a lower bound on the required normal force for the given payload. The situation when the back wheels are climbing the obstacle is similar and the above equations and framework can be extended for that case as well. The difference will arise in the moment arm vectors because when the back wheels are climbing the obstacle, the moment about the wheel ground contact point of the front wheel should be clockwise for the back wheels to climb over the obstacle.

V. CHOSSING SPRING PARAMETERS

In this section we describe the framework of choosing spring parameters for the proposed suspension mechanism. To determine the spring stiffness and damping coefficient, we first fix the maximum allowable deformation of the spring. The main condition in determining the maximum allowable deformation is that the front four-bar should not collide with the step when the spring deforms from the reaction force of the obstacle. When the front wheel comes in contact with the obstacle, the moment of the reaction forces is clockwise and hence there is a danger of the four-bar colliding with the obstacle. This is described in figure.9.

In the figure x is the minimum allowable clearance between the four-bar and the obstacle. The angle β is given by

$$\beta = \arcsin(l/(r-x)) \quad (11).$$

Since the mechanism is parallel four bar it can be easily shown that $p = (\pi/2) - \beta$ (12).

$$\text{Hence change in angle } \theta = (\pi/2) - p = \beta \quad (13)$$

Using equation (13) the spring equation can be written as

$$Ja + K_\theta \theta + cv = \tau' \quad (14),$$

where K_θ and c are the torsion spring constant and damping coefficient, $v = d\theta/dt$ and

$a = d^2\theta/dt^2$. τ' is the torque acting on the four-bar generated from the torsion spring on one of the joints and is function of the normal reaction experienced at the wheel ground contact point. J is the moment of inertia of the four-bar mechanism.

Under the assumption of gradual deformation of spring we can $a = d^2\theta/dt^2 = 0$. Hence equation (14) reduces to

$$K_\theta \theta + cv = \tau' \quad (15)$$

Equation (15) can be solved with the known information of θ as a non-linear programming problem to search for minimum values of, K_θ , c and v which satisfies the equation(15). Hence we can frame an objective function as

$$S = \min\{|K_\theta| + |c| + |v|\} \quad (16)$$

With the following constraints

$$K_\theta > 0, c > 0, v > 0 \quad (17)$$

$c = 2\sqrt{K_\theta J}$ (18) Constraint (18) represents the critical damping constraint so that there is minimum oscillation when the reaction force on the front four-bar is removed when the front wheel has climbed over the step

Table.1 shows the optimized values for the above optimization problem where τ' was estimated to be around 2.37 N-m from the considering the reaction force values and geometry of the mechanism

IV. KINEMATICS AND CLIMBING PATTERN OF THE ROVER

In this section we describe the kinematics and climbing sequence of the rover. Figure.4b,4c shows the climbing sequence of the rover. As already stated earlier when the

front wheel encounters an obstacle the four-bar deforms and produces sufficient normal force for the front wheel to climb over the obstacle. The optimum condition occurs when the instantaneous allowed direction of motion (IADM) of the wheel at any instant is almost vertical for a step-like obstacle because in this case the component of traction force along the motion direction is maximum. Referring to figure.10 when the front wheel is climbing over the obstacle the rotation centre (RC) is rear wheel ground contact point and from this reference point the instantaneous allowed direction of motion of the wheel is close to being a vertical straight line. The dotted line shows the instantaneous direction of motion (IADM) if the mechanism would have been locked configuration losing the internal mobility. When the rear wheels are encountering the obstacle the motion of the front wheels continues to advance forward stretching the torsion spring. This results in a configuration which shifts the IADM of the back wheel towards the traction force direction. This is shown in figure.11.

Table 1

Symbol	QUANTITY	Optimized value
K_θ	Torsion spring constant	8.85 N-m/radian
c	Damping coefficient	0.14N-m-s/radian
v	Rate of spring deformation	0.45rad/s
J	Moment of inertia of the four-bar	$1.1 * 10^{(-3)} \text{ N-m}^2$

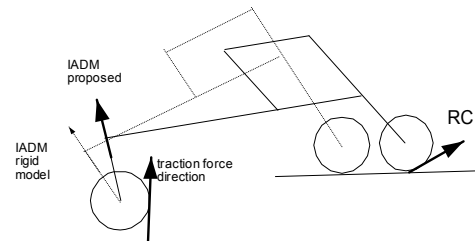


Figure.11. Instantaneous motion direction for back wheel

V. SIMULATIONS AND RESULTS

Extensive uneven terrain simulations were done using MSC Visual Nastran and MATLAB. The proposed mechanism was tested on a step like obstacle and on also on fully 3D terrain. The maximum torque and friction coefficient requirement was noted during the course of the simulation. The results presented in this section is competitive with that presented in [12] for the various other competing mechanism. The minimum coefficient of friction required is the value of the objective function (9) which is obtained online at each step while the rover is running. It represents a normalized metric which is independent of the mass of the rover and gives information about the kind of surfaces where the vehicle would be able to navigate and should not be confused with the actual coefficient of friction of the surface

which is kept constant. Figure.12a shows the average friction requirement on all the four wheels while the rover is encountering the step show in figure.4b,4c. The maximum coefficient of friction requirement goes to 0.7 momentarily when the front wheel starts climbing the obstacle. But as the ascent starts the requirement decreases. The average requirement remains mostly within 0.2-0.6 range for the entire motion periods which are highly reasonable coefficient values and comparable to that of the other suspension mechanisms described in[12]. The actual coefficient of friction of the surface was kept at 0.7 during the simulation. The peaks of the friction requirement is approximately same for both the front and rear wheels while climbing the obstacle. This shows the uniform load distribution on all the wheels which is also a desired feature for any suspension mechanism. Figure.13a gives the corresponding torque requirement for the wheels for a payload of 12 kg which directly follows from the solution of the traction forces by the optimization problem discussed in section IV. Torque requirement is an important parameter for a rover. Lower values of torque requirement will mean smaller motors decreasing the overall weight of the system. The torque requirement peak comes out to be around 3N-m for the step like obstacle. The rover was also tested on a fully 3D terrain. Figure.14 shows the rover navigating over a fully 3D terrain. Figure 12b, 15, 13b gives the coefficient of friction, slip ratio, wheel torque variation for the motion over the terrain. Figure.15 shows that for this terrain the slip ratio falls from an initial value of 0.7 to settle at the range of 0.1-0.2. The initial higher value of slip ratio is due to the initial acceleration that the rover applies to reach the desired velocity from the state of motion. Friction coefficient requirement is also fairly low for this terrain with the average being less than 0.5

VI. CONCLUSION

In this paper a novel suspension mechanism and use of passive compliance to control the internal degrees of freedom of the mechanism has been proposed. The proposed mechanism is kinematically simple since it has less number of joints and links and wheels. The mechanism performs similar to the various multi-wheeled passive suspension systems in the sense that it can climb over step-like obstacles and also navigate over irregular terrains without discontinuities.

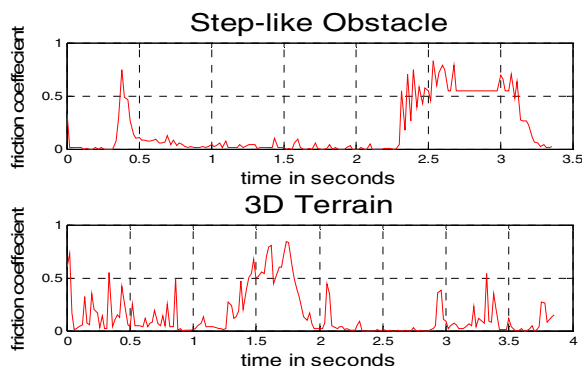


Figure.12. Variation of the friction force on the for a step like obstacle

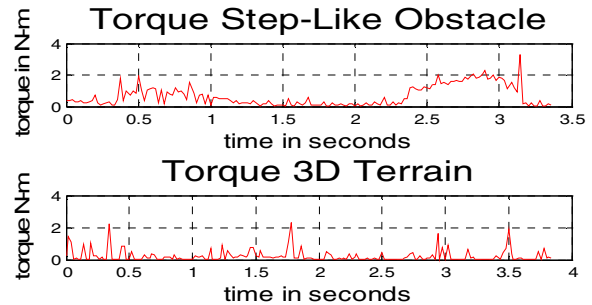


Figure.13. Wheel torques for a step like obstacle

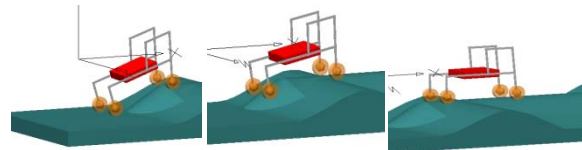


Figure.14. Rover on a fully 3D terrain

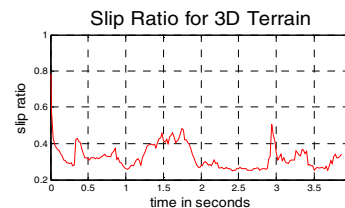


Figure.15. Variation of slip ratio

REFERENCES

- [1] R. Volpe, J. Balaram, T. Ohm and R. Ivlev, "Rocky 7: A next generation mars rover prototype," *J. Advanced Robotics*, vol. 11, no. 4, pp. 341-358, Dec. 1997.
- [2] T. Estier, Y. Crausaz, B. Merminod, M. Lauria, R. Piguet, and R. Siegwart, "An innovative space rover with extended climbing abilities," in *Proc. Int. Conf. Robotics in Challenging Environments*, Albuquerque, USA, 2000, pp.333-339
- [3] Kuroda Y, Kondok Nakamura, Kunii Y, Kubota T "Low Power Mobility System for Micro Planetary Rover "Micro5" in *Proc i-SAIRAS-99*, ESTEC Noorwidjijk, The Netherlands pp.77-82
- [4] Lunokhod-1", FTD-MT-24-1022-71, pp.66-77.
- [5] A. Eremenko et al "Rover in THE MARS-96 MISSION", Missions, Technologies and Designs of Planetary Mobile Vehicles, pp-277-300, 1992
- [6] Ch.Grand, F.Ben Amar and Ph.Bidaud "Decoupled Control of Posture and trajectory of hybrid wheel legged robot" in *Proc Int. Conference on Robotics and Automation*, New Orleans, LA, 2004, vol 5, pp.5111-5116
- [7] I.Han "Development of stair climbing robot with springs and planetary wheels" in *Journal of Mechanical Engineering Sciences*, I-Mech Vol 222 No 7, pp.1289-1296
- [8] Ambrose Krebs, Thomas Thueer, Stephane Michaud and Roland Siegwart "Performance Optimisation of All Terrain Rovers-A 2D Qui-Static Tool" in *Proc of the IEEE/RSJ International Conference on Intelligent Robots and Systems*, IROS-2006, pp.4266-4271
- [9] Arun Kumar Singh, Vijay Eathakota, K.Madhava Krishna and Arun.H.patil "Evolution of four-wheeled active suspension with minimal actuation for rough terrain mobility" in *Proc Int. Conference on Robotics and Bio-mimetics ROBIO-2009*, Guilin, China, pp.794-799
- [10] J.J.Craig "Introduction to Robotics-Mechanics and Control"-Third Edition Prentice Hall
- [11] Seung Kook Jun, Glen D White, Venkat Krovi, "Kinetostatic Design Consideration for an Articulated Leg-Wheel Locomotion Subsystem" in *ASME Journal of Dynamic System, Measurement and Control*, March-2006 VOL-128 pp.112-121
- [12] Thomas Thueer, A.Krebs, Roland Siegwart "Comprehensive locomotion performance evaluation for all terrain robots" *IROS-06*